High- and Low-Pitch Helical Structures of Tilted Chiral Lipid Bilayers

Shigeyuki Komura[1] and Ou-Yang Zhong-can[1,2]
[1]*Faculty of Computer Science and Systems Engineering, Kyushu Institute of Technology, Iizuka 820, Japan*
[2]*Institute of Theoretical Physics, Academia Sinica, P.O. Box 2735, Beijing 100080, China*
(Received 13 November 1997)

Molecular packing in helical ribbons of tilted chiral lipid bilayers is investigated as cholesteric liquid crystals. Two types of helices with high- and low-pitch angles observed in the pathway for cholesterol crystallization (ChC) in native and model biles by Chung *et al.* [Proc. Natl. Acad. Sci. U.S.A. **90**, 11 341 (1993)] correspond to parallel and antiparallel packing of molecules at the edges of the ribbon, respectively. The structural change in the ChC is explained as a decreasing succession of free energy of the metastable intermediate structures. [S0031-9007(98)06588-0]

PACS numbers: 87.10.+e, 61.30.–v, 68.15.+e, 87.22.Bt

Tubular and helical structures are rather commonly observed in nature [1]. For example, many authors found various helical structures of chiral lipid bilayers (CLBs) in recent experiments [2]. Among several theoretical approaches, a fundamental basis which is consistent with the experiments is that the molecular packing interaction is chiral as in cholesteric liquid crystals (ChLCs) [3–5]. According to the early theories, the pitch angle of the helix [ϕ_0 in Fig. 1(a)] has been predicted to be 45° which is in good agreement with the previous experimental observations [2].

Although the concept of molecular packing interaction in ChLCs has been experimentally confirmed [6] and theoretically extended [7,8], a recent challenge is to understand the new findings in cholesterol crystallization in native and model biles [9,10]: Micellar model biles composed of bile salt sodium taurocholate, lecithin, and cholesterol in a molar ratio of 97.5:0.8:1.7 were initially prepared and contained both micelles and vesicles. Within 2–4 hours of dilution, filamentous structures were observed. A few days later, the filaments were bent to form high-pitch helices [≈54°, Fig. 2(a) in [10]]. These helices grew laterally while maintaining the pitch angle to form tubules [Fig. 2(b) in [10]]. Within a few weeks, high-pitch helices and tubules disappeared, while new helices with low-pitch angle (≈11°) appeared and grew to form new tubules [Figs. 2(c) and 2(d) in [10]]. Eventually only platelike cholesterol monohydrate crystals (ChMs) remained [Figs. 2(e) and 2(f) in [10]]. One of their interesting findings is the existence of helical ribbon structures with two distinctive pitch angles: high- (54°) and low-pitch (11°) helices. To explain these structures, Chung *et al.* [10] used a previous theory [11] appropriate for anisotropic bilayers of tilted chiral amphiphiles case and derived a free energy per unit area as

$$g = (1/2\rho_0^2)[k^{cc}\cos^4\phi_0 + k^{pp}\sin^4\phi_0 + (k^{cp}/2)\sin^2 2\phi_0] - (k^*/2\rho_0)\sin 2\phi_0, \quad (1)$$

where ρ_0 and ϕ_0 are radius and pitch angle of the helical ribbon, respectively (see Fig. 1); k^{cc}, k^{pp}, k^{cp}, and k^* are elastic constants. For the equilibrium helix, they obtained the relation $\tan\phi_0 = (k^{cc}/k^{pp})^{1/4}$. Corresponding to $\phi_0 = 54°$ and 11°, the calculated ratio is $k^{cc}/k^{pp} =$ 3.4 and 0.0015, respectively. However, as commented very recently by Selinger *et al.* [12], the ratio of 3.4 is reasonable, but that of 0.0015 is surprising. For this reason, Selinger *et al.* assumed that the molecular tilt direction (**m** in Fig. 1) varies linearly across the ribbon

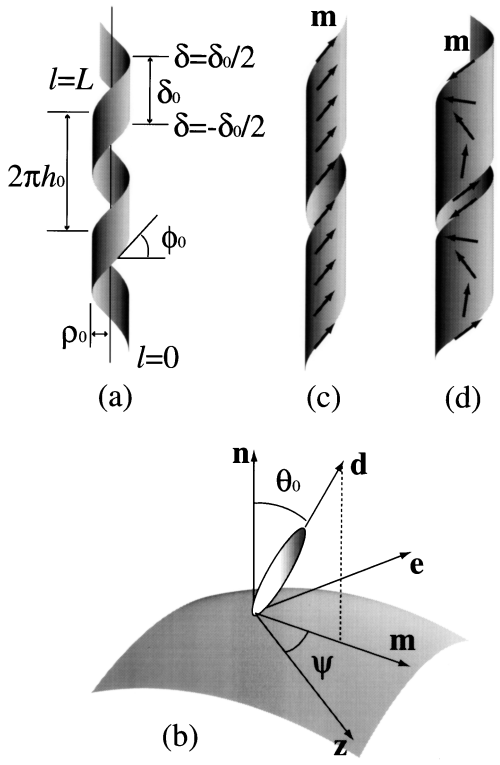

FIG. 1. Schematic illustration of the helical ribbon: (a) the geometric parameters characterizing the ribbon; (b) local coordinate system of TCLB; (c) helical ribbon with parallel packing of molecules (P-helix); (d) helical ribbon with antiparallel packing of molecules (A-helix).

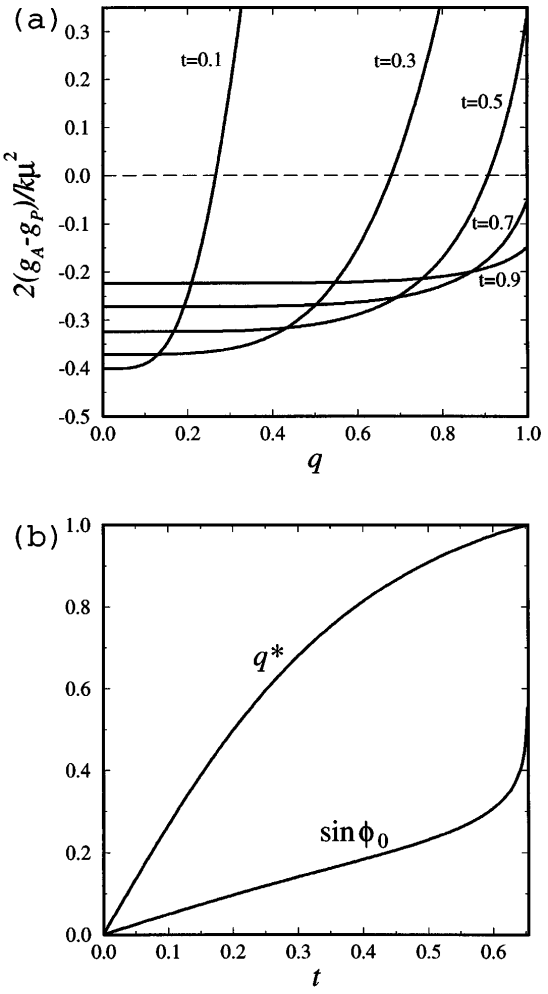

FIG. 2. (a) $2(g_A - g_P)/k\mu^2$ versus q for several values of $t = \tan\theta_0$ and (b) q^* and $\sin\phi_0$ versus $t = \tan\theta_0$ for $0 < \theta_0 < \theta_0^*(\tan\theta_0^* \simeq 0.654)$, respectively.

[12]. Although the observed low-pitch angle 11° has been attributed to the difference between the helical direction and the tilt direction in their paper, there is no evidence for the linear ansatz and the theory has not yet reached the conclusive explanation on the existence of two types of helices. Thus, the general question can be posed as follows: What is the nature of the existence of two types of helices, and can we theoretically discuss the above sequence of transition as well as each structure from the energetic point of view?

In this Letter, we investigate the molecular packing on a helical ribbon of CLBs as ChLCs by generalizing our previous theory [4]. In Ref. [4], we employed only $g_{ch} = -k_2\mathbf{d}\cdot\nabla\times\mathbf{d}$ as an energy, where $\mathbf{d}$ is a unit vector parallel to the long axis of the molecules [see Fig. 1(b)] and k_2 characterizes the chirality of ChLC. With this simplified energy, the pitch angle was predicted to be 45°. Here we give a calculation by using the complete free energy density per unit area of ChLC [13]

$$g_{\mathrm{LC}} = \frac{k_{11}}{2}(\nabla\cdot\mathbf{d})^2 + \frac{k_{22}}{2}\left(\mathbf{d}\cdot\nabla\times\mathbf{d} - \frac{k_2}{k_{22}}\right)^2 + \frac{k_{33}}{2}(\mathbf{d}\times\nabla\times\mathbf{d})^2, \quad (2)$$

where k_{ii} ($i = 1, 2,$ and 3) are the splay, twist, and bending elastic constants, respectively, and ∇ is the three-dimensional gradient operator. To view (2) as an energy per unit area, we regard k_{ii} and k_2 as the corresponding elastic constants of ChLC multiplied by the thickness of the CLB, and thence the total free energy of the CLB is given by $F = \oint g_{\mathrm{LC}}\,dA$, where dA is the area element of the CLB surface. We allow the molecular tilt direction $\mathbf{m}$ (see below for the definition) to vary on the bilayer as proposed by Selinger *et al.* [5,12], but keep the boundary condition that the tilt direction is aligned with the helical direction at the ribbon edges. The latter condition has been also considered in the previous theories [3,7,10] and confirmed by x-ray diffraction studies [14]. Especially, instead of assuming a simple linear ansatz for the tilt direction field [12], we obtain it exactly by solving the Euler-Lagrange equation derived from g_{LC}. With these refinements, we will reveal that for the high-pitch helices, molecules at the two edges of bilayers tilt parallel with each other [Fig. 1(c)], whereas for the low-pitch helices, they tilt antiparallel with each other [Fig. 1(d)]. Helix formation takes place through a transition from a fluid CLB (chain-melted L_α) phase to a tilted CLB (TCLB, chain-frozen L_{β^*}) phase under cooling or dilution [6]. The observed sequence of structures from filaments to ChMs by way of two types of helices can be shown as a decreasing succession of free energy of the metastable intermediate structures and regarded as a quenchlike cooling process of the molecular tilt.

Mathematically, a surface of a helical ribbon wound around a cylinder of radius ρ_0 can be represented by a vector function with two variables as $\mathbf{Y}(\ell,\delta) = (\rho_0\cos\omega_0\ell, \rho_0\sin\omega_0\ell, h_0\omega_0\ell + \delta)$, where $\omega_0 = 1/\sqrt{\rho_0^2 + h_0^2}$ [see Fig. 1(a)]. The pitch angle and the pitch of the helix are given by $\phi_0 = \arctan(h_0/\rho_0)$ and $2\pi|h_0|$, respectively. Moreover, ℓ and δ satisfy $0 \le \ell \le L$ and $-\delta_0/2 \le \delta \le \delta_0/2$, respectively, where L is the arc length along the edge of the ribbon, and δ_0 is the ribbon width along the z axis (the central axis of the cylinder). We introduce the tilt of the director field by $\mathbf{d} = \cos\theta_0\mathbf{n} + \sin\theta_0\mathbf{m}$, where $\mathbf{n}$ is the unit normal vector of the ribbon surface, $\mathbf{m}$ is the unit vector parallel to the projection of $\mathbf{d}$ on the surface, and the tilt angle θ_0 is the angle between $\mathbf{n}$ and $\mathbf{d}$ [see Fig. 1(b)] [11]. θ_0 characterizes the transition from the fluid (L_α) phase with $\theta_0 = 0$ to the TCLB (L_{β^*}) phase with a constant $\theta_0 > 0$. Generally, $\mathbf{m}$ can be written in terms of single angle $\psi(\ell,\delta)$ as $\mathbf{m} = \cos\psi(\ell,\delta)\mathbf{z} + \sin\psi(\ell,\delta)\mathbf{e}$, where $\mathbf{z}$ is the unit vector along the z axis and $\mathbf{e}$ is the unit vector along the circumference of the cylinder.

For simplicity but without loss of generality, we consider the case where ψ is a function of only δ, and use the one-constant approximation, i.e., $k_{11} = k_{22} = k_{33} = k$. Then (2) becomes [15]

$$g_{\mathrm{LC}} = (k/2\rho_0^2)[\cos^2\theta_0 + \sin^2\theta_0(4\sin^2\psi + \omega_0^{-2}\psi_\delta^2) - \sin 2\theta_0(h_0\cos\psi + \rho_0\sin\psi)\psi_\delta] - (k_2/2\rho_0)[\sin 2\theta_0(h_0\sin\psi - \rho_0\cos\psi)\psi_\delta + 2\sin^2\theta_0\sin 2\psi] + k\mu^2/2, \quad (3)$$

where $\psi_\delta = d\psi/d\delta$, and $\mu = k_2/k$ is the inverse of the pitch of ChLC [4,13]. For constant ψ, one can show that (3) coincides with (1) when $k^{pp} = k\cos^2\theta_0$, $k^{cc} = k(\cos^2\theta_0 + 4\sin^2\theta_0)$, $k^{cp} = k\cos^2\theta_0$, and $k^* = 2k_2\sin^2\theta_0$, except the constant term. Progress in the present work is to consider the case without the constraint of constant ψ. We therefore derive the Euler-Lagrange equation from (3) as

$$\psi_{\delta\delta} = 2\omega_0^2\sin(2\psi - \alpha_0)/\cos\alpha_0, \quad (4)$$

where $\psi_{\delta\delta} = d^2\psi/d\delta^2$ and $\alpha_0 = \arctan(\mu\rho_0)$. The general form of the first integral of (4) is

$$\psi_\delta = (2\omega_0/\sqrt{\cos\alpha_0})\sqrt{\cosh^2 C - \cos^2(\psi - \alpha_0/2)}, \quad (5)$$

where C is an integral constant.

Obviously, Eq. (4) has a constant solution of $\psi = \psi_0 = \alpha_0/2$, and we let $\phi_0 = \pi/2 - \psi_0 = \pi/2 - \alpha_0/2$ to satisfy the boundary condition such that the molecules at the two edges of the ribbon tilt parallel with each other. We call this configuration "parallel packing" (P-helix) as shown in Fig. 1(c). It is necessary to check whether such a helix is in mechanical equilibrium or not. We then define the curvature κ_0 and the torsion τ_0 of the helix by $\kappa_0 = \rho_0\omega_0^2$ and $\tau_0 = h_0\omega_0^2$, respectively. Then the elastic energy of the P-helix is expressed from (3) in terms of κ_0 and τ_0 as $g_P = (k/2)[4\sin^2\theta_0(\kappa_0^2 + \tau_0^2) + \cos^2\theta_0(\kappa_0 + \tau_0^2/\kappa_0)^2] - 2k_2\tau_0\sin^2\theta_0 + k\mu^2/2$. Minimizing this with respect to κ_0 and τ_0, i.e., $\partial g_P/\partial\kappa_0 = \partial g_P/\partial\tau_0 = 0$, we obtain the optimal geometry of the helical ribbon characterized by

$$\tan\phi_0 = (1 + 4\tan^2\theta_0)^{1/4}, \quad (6)$$

$$\mu\rho_0 = -\tan 2\phi_0 = \frac{2(1 + 4\tan^2\theta_0)^{1/4}}{(1 + 4\tan^2\theta_0)^{1/2} - 1}, \quad (7)$$

and the corresponding energy per unit area is $g_P = k\mu^2/2$. These results reveal some important features of the P-helix. First, we note that (7) is identical to the assumed boundary condition, $\phi_0 = \pi/2 - \alpha_0/2$ with $\alpha_0 = \arctan(\mu\rho_0)$, and hence the calculation is self-consistent. This confirms the helix being in mechanical equilibrium since the minimization condition requires the state of both free external force and moment. Second, the result of (6) essentially corresponds to that by Chung *et al.* as mentioned before (note also the relations between k^{cc}, k^{pp}, and k), and predicts a high-pitch angle of $\phi_0 > \pi/4$. We have also performed the minimizing calculation without using the one-constant approximation and obtained an equation as $\cos^2 2\phi_0 + [2 + (k_{11}/k_{33})\cot^2\theta_0]\cos 2\phi_0 + 1 = 0$. Since this equation possesses a negative solution for $\cos 2\phi_0$, we can show $\phi_0 > \pi/4$ as before, and it reduces to (6) when $k_{11} = k_{33}$. Third, since the radius ρ_0 is inversely proportional to the chiral elastic constant k_2, we see that the origin of the cylindrical curvature is due to the chirality of molecules. In fact, (7) reveals that the pitch (μ^{-1}) should be proportional to the radius. This is one of the remarkable facts observed in experiments (see Figs. 4–6 in Ref. [10]).

According to the experiments, a straight filament appears at the initial stage of the crystallization process in model biles and can be identified as $\rho_0 = 0$ [9]. This fact indicates that the initial stage of the TCLB helix is quenched to the structure with $\phi_0 = \pi/2$ [notice (7) and $\phi_0 > \pi/4$]. From (6), one can then expect that the tilt angle takes the maximum value $\theta_0 = \pi/2$. After the quench, θ_0 will decrease from $\pi/2$ to its stable value and the straight filaments will bend and twist by decreasing ϕ_0 and increasing ρ_0 [9,10]. This is the expected mechanism underlying the transition from the straight filaments to the high-pitch helices.

We now turn to consider the case where the tilt direction can vary on the bilayer across the ribbon. Since the tilt direction coincides with the helical direction at the ribbon edges, the allowed boundary condition for the nonuniform solution is $\psi(-\delta_0/2) = \pi/2 - \phi_0$ and $\psi(\delta_0/2) = \psi(-\delta_0/2) + \pi = 3\pi/2 - \phi_0$. The molecular configuration subjected to this boundary condition is called "antiparallel packing" (A-helix) and is depicted in Fig. 1(d). We will show below that the helical structure produced from the antiparallel packing of molecules indeed results in the low-pitch angle. The integral constant C in (5) is now determined by the boundary condition as $\delta_0 = \sqrt{\cos\alpha_0}\,qK(q)/\omega_0$ with $q = 1/\cosh C$, whereas the energy per unit area can be calculated from (3) as [15]

$$g_A = (k\mu^2/2)[1 + (1 + \sin^2\theta_0)x^2 + 2\sin^2\theta_0 x\sqrt{1 + x^2}\,(1 - 2/q^2) + 8\sin^2\theta_0 x\sqrt{1 + x^2}\,E(q)/q^2K(q) - 2\sin 2\theta_0\sqrt{x}\,(1 + x^2)^{1/4}/qK(q)], \quad (8)$$

where $x = \cot\alpha_0$; $K(q)$ and $E(q)$ are the first and second complete elliptic integrals given by $K(q) = \int_0^{\pi/2} d\varphi/\sqrt{1 - q^2\sin^2\varphi}$ and $E(q) = \int_0^{\pi/2} d\varphi\sqrt{1 - q^2\sin^2\varphi}$, respectively. To ensure that the helix is in mechanical

equilibrium we must minimize g_A. Because q is a function of δ_0, ϕ_0, and α_0, minimization of g_A over these quantities leads simultaneously to $\partial g_A/\partial q = 0$. From this and with the help of differential relations, $dK(q)/dq = [E(q)/q(1-q^2)] - K(q)/q$ and $dE(q)/dq = [E(q) - K(q)]/q$, we can obtain the relation between α_0 and q as $\sqrt{\cos\alpha_0}/\sin\alpha_0 = q\cot\theta_0/2E(q)$. By substituting this into (8), g_A then becomes

$$g_A = (k\mu^2/2)[1 + (1 + \sin^2\theta_0)(\sqrt{1 + 4y^4} - 1)/2 + 2y^2\sin^2\theta_0 - \cos^2\theta_0/E^2(q)], \quad (9)$$

where $y = \sqrt{\cos\alpha_0}/\sin\alpha_0$ [$\alpha_0 = \arctan(\mu\rho_0)$ as before].

In Fig. 2(a) we have plotted scaled $g_A - g_P$ as a function of q for several values of $t = \tan\theta_0$. There exists a critical value of θ_0 (denoted as θ_0^*) such that for $0 < \theta_0 < \theta_0^*$ there exists a critical value of q (denoted as q^*) at which g_P is equal to g_A, whereas for $\theta_0^* < \theta_0 < \pi/2$, g_A is always smaller than g_P predicting the transition from P-helix to A-helix. In Fig. 2(b), q^* is plotted against $t = \tan\theta_0$ for $0 < \theta_0 < \theta_0^*$. θ_0^* can be obtained by solving $g_P = g_A$ at $q = 1$ and is $\tan\theta_0^* \simeq 0.654$. If we consider the case when the helix closes to form a tube ($\delta_0 = 2\pi h_0$), then $\delta_0 = (2\pi/\mu)\tan\alpha_0\tan\phi_0$ holds. With this relation, we can calculate the pitch angle of the helix as

$$\sin\phi_0 = \frac{K(q)}{2\pi}[\sqrt{q^4 + 4\tan^4\theta_0 E^4(q)} - 2\tan^2\theta_0 E^2(q)]^{1/2}. \quad (10)$$

In Fig. 2(b), we have also plotted $\sin\phi_0$ versus $t = \tan\theta_0$ with $q = q^*$. Except at the singular point $\theta_0 = \theta_0^*$, this graph generally shows $\phi_0 < 30°$ indicating that the antiparallel packing results in the low-pitch angle. This is one of the important results of this paper.

Another interesting feature is that for each curve in Fig. 2(a), we see that $q = 0$ gives the minimum of g_A, and hence it is the unique stable state. The state $q = 0$ leads to $\alpha_0 = \pi/2$ which corresponds to $\rho_0 \to \infty$ since $\alpha_0 = \arctan(\mu\rho_0)$. In fact, this result confirms the observation in experiments. At the final stage of the crystallization process, the tubes fracture at their ends to produce platelike ChMs (see Fig. 2 in Ref. [10]). In other words, P-helix or A-helix are metastable intermediates although they are static solutions of the Euler-Lagrange equation (4).

As a progress compared to the previous theories [10,12], Fig. 2(a) predicts an important fact that the transition from the low-pitch helices (A-helix) to the ChMs can be continuous while that from the high-pitch helices (P-helix) to the ChMs is discontinuous. All the curves for $g_A(q)$ are continuous and have their minima at $q = 0$. This feature indicates that the helical tubes of the low-pitch angle transform continuously into platelike ChMs as shown in Fig. 2(f) in Ref. [10]. For the high-pitch helices, the dissolution process is necessary to transform into the ChMs [10]. Since the energy for ChMs ($q = 0$) is $g_{\mathrm{ChM}} = (k\mu^2/2)[1 - (2/\pi)^2\cos^2\theta_0]$, $g_P = k\mu^2/2$ is always larger than g_{ChM} except for $\theta_0 = \pi/2$. This fact explains why the initial stage of the helical structures of TCLB is quenched to $\theta_0 = \pi/2$ as mentioned before. The experimental observations confirm very well the above predictions [10].

This consideration now leads us to determine the optimal high-pitch angle. For the transition from the high-pitch helices to the ChMs, θ_0 must reduce to θ_0^* in order to satisfy the condition $g_P = g_A$ from which the branch of low-pitch helix starts in Fig. 2(a). Hence the optimal high-pitch angle is precisely obtained from (6) as [15]

$$\phi_0 = \arctan\left\{\left[\frac{8}{3}\cos\left(\frac{1}{3}\arccos\frac{5}{32}\right) + \frac{1}{3}\right]^{1/4}\right\} \simeq 52.1°, \quad (11)$$

which is in excellent agreement with the experimentally observed value $\phi_0 = 53.7 \pm 0.8°$ [10].

This work is supported by the Ministry of Education, Science and Culture, Japan (Grant-in-Aid for Scientific Research No. 09740318).

[1] For a review, see J. M. Schnur, Science **262**, 1669 (1993).
[2] N. Nakashima *et al.*, Chem. Lett. **1984**, 1709 (1984); P. Yager and P. E. Schoen, Mol. Cryst. Liq. Cryst. **106**, 371 (1984); N. Nakashima *et al.*, J. Am. Chem. Soc. **107**, 509 (1985); J. H. Georger *et al.*, J. Am. Chem. Soc. **109**, 6169 (1987); J.-H. Fuhrhop *et al.*, J. Am. Chem. Soc. **110**, 2861 (1988).
[3] W. Helfrich and J. Prost, Phys. Rev. A **38**, 3065 (1988).
[4] Ou-Yang Zhong-can and Liu Jixing, Phys. Rev. Lett. **65**, 1679 (1990); Phys. Rev. A **43**, 6826 (1991).
[5] J. V. Selinger and J. M. Schnur, Phys. Rev. Lett. **71**, 4091 (1993).
[6] B. N. Thomas *et al.*, Science **267**, 1635 (1995).
[7] J. S. Chappell and P. Yager, Chem. Phys. Lipids **58**, 253 (1991).
[8] P. Nelson and T. Powers, Phys. Rev. Lett. **69**, 3409 (1992).
[9] F. M. Konikoff *et al.*, J. Clin. Invest. **90**, 1155 (1992).
[10] D. S. Chung *et al.*, Proc. Natl. Acad. Sci. U.S.A. **90**, 11 341 (1993).
[11] I. Dahl and S. T. Lagerwall, Ferroelectrics **58**, 215 (1984).
[12] J. V. Selinger, F. C. MacKintosh, and J. M. Schnur, Phys. Rev. E **53**, 3804 (1996).
[13] P. G. de Gennes and J. Prost, *The Physics of Liquid Crystals* (Clarendon, Oxford, 1993), 2nd ed.
[14] M. Caffrey *et al.*, Biochemistry **30**, 2134 (1991).
[15] The details will appear in a full paper by the authors.